Journal of Iron and Steel Research, International 24 (2017) 1231－1237

Contents lists available at ScienceDirect

Journal of Iron and Steel Research, International

journal homepage: www.chinamet.cn

Effect of martensitic transformation on nano/ultrafine-grained structure in 304 austenitic stainless steel

Na Gong[1], Hui-bin Wu[1,2,*], Gang Niu[2], Jia-ming Cao[1], Da Zhang[1], Tana[3]

[1] Institute of Engineering Technology, University of Science and Technology Beijing, Beijing 100083, China

[2] Collaborative Innovation Center of Steel Technology, University of Science and Technology Beijing, Beijing 100083, China

[3] Sinohydro Renewable Energy Co., Ltd., Beijing 100083, China

ARTICLE INFO

Key words:
304 austenitic stainless steel
Nano/ultrafine-grained structure
Reversion mechanism
Lath-type martensite
Dislocation-cell type martensite
Martensitic transformation

ABSTRACT

304 austenitic stainless steel was cold rolled in the range of 20%－80% reductions and then annealed at 700－900 ℃ for 60 s to obtain nano/ultrafine-grained (NG/UFG) structure. Transmission electron microscopy, electron backscatter diffraction and X-ray diffraction were used to characterize the resulting microstructures. The results showed that with the increase of cold reduction, the content of martensite was increased. The steel performed work hardening during cold-working owing to the occurrence of strain induced martensite which nucleated in single shear bands. Further rolling broke up the lath-type martensite into dislocation-cell type martensite because of the formation of slip bands. Samples annealed at 800－960 ℃ for 60 s were of NG/UFG structure with different percentage of nanocrystalline (60－100 nm) and ultrafine (100－500 nm) grains, submicron size (500－1000 nm) grains and micron size (>1000 nm) grains. The value of the Gibbs free energy exhibited that the reversion mechanism of the reversion process was shear controlled by the annealing temperature. For a certain annealing time during the reversion process, austenite nucleated first on dislocation-cell type martensite and the grains grew up subsequently and eventually to be micrometer/submicrometer grains, while the nucleation of austenite on lath-type martensite occurred later resulting in nanocrystalline/ultrafine grains. The existence of the NG/UFG structure led to a higher strength and toughness during tensile test.

1. Introduction

Austenitic stainless steel (SS) is quite suitable for structural applications due to its excellent corrosion characteristic, but because of the lack of high strength, it is hard to apply in construction fields widely[1]. Grain refinement is supposed to be a potential method in developing the strength of the materials[2,3]. Thermomechanical controlled processing (TMCP) is considered to be one of the primary methods to realize the exact grain refinement. It was reported that TMCP together with microalloying elements such as element Nb got the grain size of ferrite down to 4－5 μm in body-centered cubic (bcc) ferrous alloys[4-6]. However, generally TMCP results in coarse grain size to 20－40 μm based on the processing condition in austenitic stainless steel. Besides, it is not effective. Olson and Cohen[7] proposed a model to account for strain induced martensite (SIM) formation because of cold deformation. However, many studies proved that the martensitic morphology comprised dislocation forests, walls and tangles, and incidental dislocation boundaries, and was severely deformed lath-type martensite and dislocation cell-type martensite in cold deformed low-carbon steel, specialty steels and Fe-Cr-Ni alloys[8-13].

Recently, several kinds of austenitic stainless steels such as 304, 304L, and 316L were subjected to heavy cold deformation and reversion transformation to develop nano/ultrafine-grained (NG/UFG) structure[14-16]. Regarding this matter, a method which is gaining wide acceptance for improving the strength of austenitic stainless steel without degrading ductility is to anneal a heavily cold deformed metastable austenitic stainless steel to produce NG/UFG structure[10,17-19]. And thermomechanical reversion treatment on the basis of SIM transforma-

* Corresponding author. Prof., Ph.D; Tel.:+86 10 62332617.
E-mail address: *wuhb@ustb.edu.cn* (*H.B. Wu*).

Received 12 November 2016; Received in revised form 26 April 2017; Accepted 9 May 2017
Available online 15 December 2017

tion has been regarded as a quite significant approach to obtain NG/UFG structure in austenitic SS[20-25]. It is shown that the structure of NG/UFG can add a lot in toughness while just very small dip in strength[2,3,26]. Severe cold rolling of austenite makes austenite (fcc γ) grain transform to martensite (bcc α′) under the condition of room temperature. It was reported that SIM reverted to austenite either by shear controlled or diffusion controlled mechanism during reversion treatment[14,19,26,27]. Based on different fractions of cold rolling and annealing temperature-time arrangement, different good combination of good strength and toughness can be obtained[14]. In this research, emphasis was laid on the effect of martensitic transformation on NG/UFG structure in 304 SS. Meanwhile, a grain size distribution statistic was done to quantitatively describe the nano/ultrafine grains.

2. Material and Methods

A commercial 304 SS in the form of a sheet with thickness of 7.9 mm was used as the initial material. The composition of the 304 SS is Fe-0.04C-0.16Si-1.52Mn-17.8Cr-8.1Ni-0.005P-0.005S. The samples were heated to 1050 ℃ and held for 12 min to solution treatment. The initial austenite grain size was in the range of 20—40 μm with single-phase of austenite as shown in Fig. 1. Several specimens with dimensions of 600 mm×80 mm were prepared for cold rolling (CR). CR was set at reductions of 20%—80% at room temperature. Simulated annealing experiment was carried out on CCT-AV-II simulated annealing experiment machine. The specimens were heated at a heating rate of 30 ℃/s and then annealed at 700—900 ℃ for 60 s with a cooling rate of 50 ℃/s.

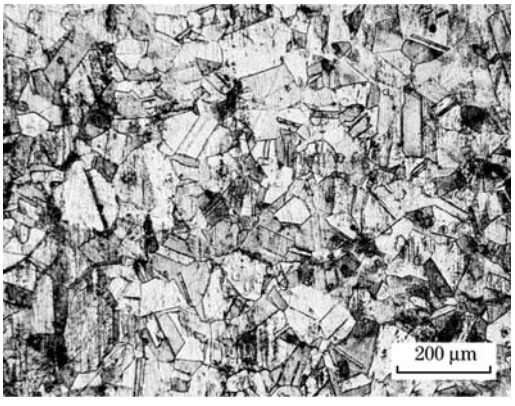

Fig. 1. Initial grain structure after solution treatment of 304 SS.

The microstructural evolutions were analyzed using the optical microscope (Zeiss Axiovert 40MAT), and transmission electron microscope (TEM, Tecnai G2 F30 S-TWIN). X-ray diffraction (XRD) measurements (Rigaku DMAX-RB with CuKα radiation) were employed to identify the phases. The electron backscatter diffraction (EBSD) was applied to determine the microscopic characterization. Before XRD and EBSD, the specimens were prepared by electropolishing at a voltage of 15 V for 30 s, and the electrolyte contained 20 vol. % of perchloric acid and 80 vol. % of ethanol. The tensile tests were carried out at room temperature using the CMT5605 tensile machine. And Vickers micro-hardness values were measured on HV-1000 micro-Vickers durometer.

3. Results and Discussion

Fig. 2 shows XRD patterns of the different cold deformed specimens from the initial specimen (0% CR) to 80% reduction. The initial sample consists of single-phase of austenite with $(211)_\gamma$, $(110)_\gamma$ and $(200)_\gamma$ peaks with the austenite content of 100%, as shown in Fig. 2. It can be seen that with the increase of cold reduction, the content of martensite is increased, while the content of austenite is decreased, observed from the peak intensities in X-ray diffraction. The volume fractions of the martensite phases were calculated using MDI Jade 5.0 based on the XRD results. It is worth noting that after 80% CR, there are two peaks of α′ martensite, namely $(200)_M$ and $(211)_M$ peaks with the high content of SIM 83.2%.

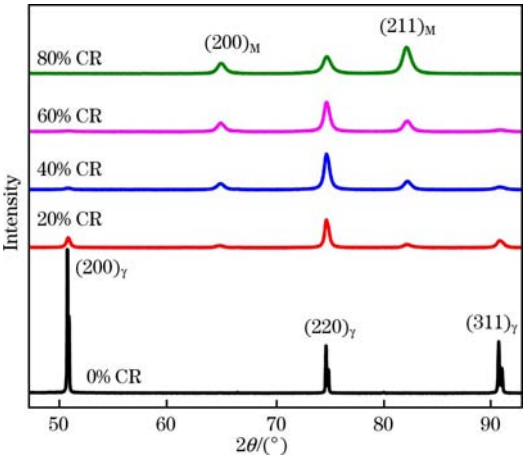

Fig. 2. X-ray diffraction patterns of the cold rolled 304 SS.

The stress-strain results of specimens with different cool rolling reductions are shown in Fig. 3. It clearly demonstrates the effect of rolling on the shape of the stress-strain curves of 304 SS. With the increase of cold rolling, the plastic deformation of the steel is known. The mechanical properties with different reductions of CR are shown in Table 1. With the increase of cold rolling, the strength and hardness of the steel are increased, while the elongation to failure is decreased. Furthermore, it is known that the initial specimen exhibits a low yield strength (YS) of (253±22) MPa, the ultimate tensile strength (UTS) of (733±25) MPa and great elongation (EL) of 69.8%±2%. With 20% CR, the hardness

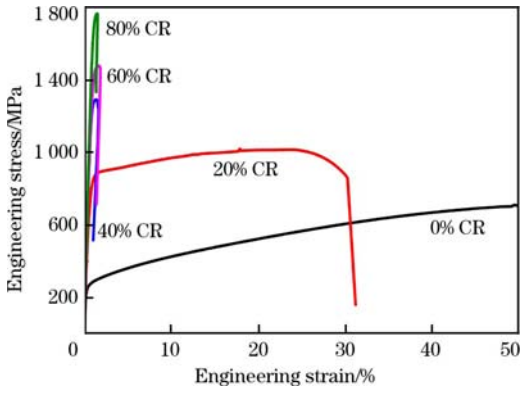

Fig. 3. Engineering stress-strain tensile data for the cold rolled 304 SS.

Table 1
Mechanical properties for the cold rolled 304 SS

Cold reduction/%	UTS/MPa	YS/MPa	EL/%	Hardness/HV
0	733±25	253±22	69.8±2	183±3
20	1024±30	720±20	31.4±1.5	342±8
40	1276±35	1187±40	8.6±3	413±9
60	1476±22	1371±50	5.3±3	450±10
80	1762±28	1694±30	2.5±2.5	504±7

changes from (183±3) HV to (342±8) HV. It is suggested that small deformation produces large work hardening. After 80% CR, the YS is largely increased to (1694±30) MPa, which is approximately over six times higher than that of the initial one, with quite low ductility of 2.5%±2%. What's more, it is also indicated that the gap between the yield strength and tensile strength curves becomes narrower with the increase of cold rolling as shown in Table 1. Consequently, it is found that austenitic stainless steel performs work hardening during cold-working and this kind of work hardening may be attributed to the formation of martensite.

TEM micrographs of initial sample are shown in Fig. 4. Many kinds of stacking faults, twins and dislocations can be observed in Fig. 4. Fig. 5(a) shows TEM micrograph of sample cold rolled with 20% reduction. Single shear bands without any intersection are observed in this sample. It was reported in the studies of Lee and Lin[28] that the formation of martensite occurred via repeating nucleation and coalescence and finally generated to long martensite lathes. The mechanism was considered to be the most authoritative explanation since studies showed that the martensite nuclei were formed in the place of shear band[29]. Fig. 5(b) shows TEM image of the 40% cold-rolled specimen. It seems that a few remaining austenite regions appear as circled in Fig. 5(b). It is thought that saturation state can be reached only under enough cold deformation. And then further deformation broke the structure and therefore resulted in smaller size of martensite. Further deformation produces enough energy together with nucleation sites for reversion transformation to gain the NG/UFG structure. Thus, it is likely that 40% deformation is not yet enough to create sufficient nucleation sites.

TEM images of 80% cold rolling are shown in Fig. 6. As shown in Fig. 6(a), uniform lath-type martensite extends in the direction of CR with the measured width to be about 100 nm, which is smaller than that of sample with 40% reduction. Comparing Figs. 6(a) and 6(b), they are all named martensite structure. However, lath-type martensite is shown in Fig. 6(a) while deformation-cell type martensite is shown in Fig. 6(b). Reports have shown that further rolling under saturation state breaks up the lath-type martensite into finer lathes and ultimately the dislocation-cell type martensite because of the formation of slip bands[10,29-32]. However, Misra et al.[30]

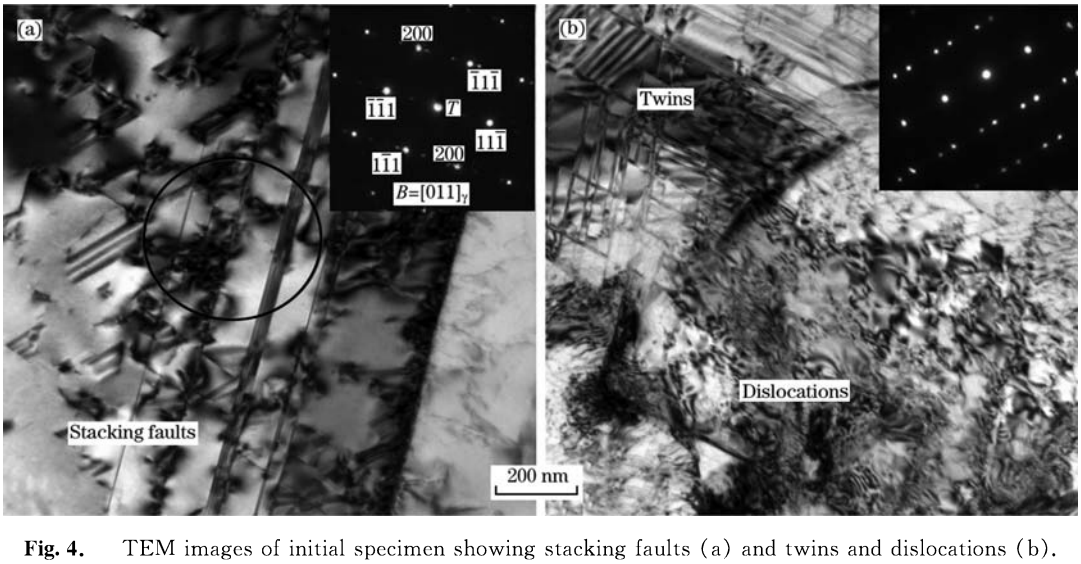

Fig. 4. TEM images of initial specimen showing stacking faults (a) and twins and dislocations (b).

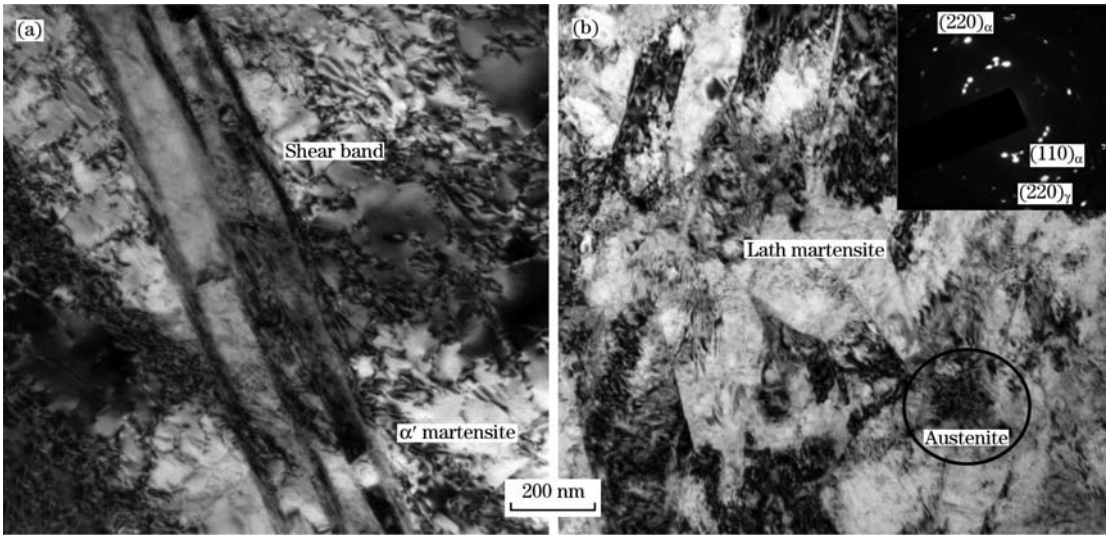

Fig. 5. TEM images of cold rolled specimen showing 20% (a) and 40% CR (b).

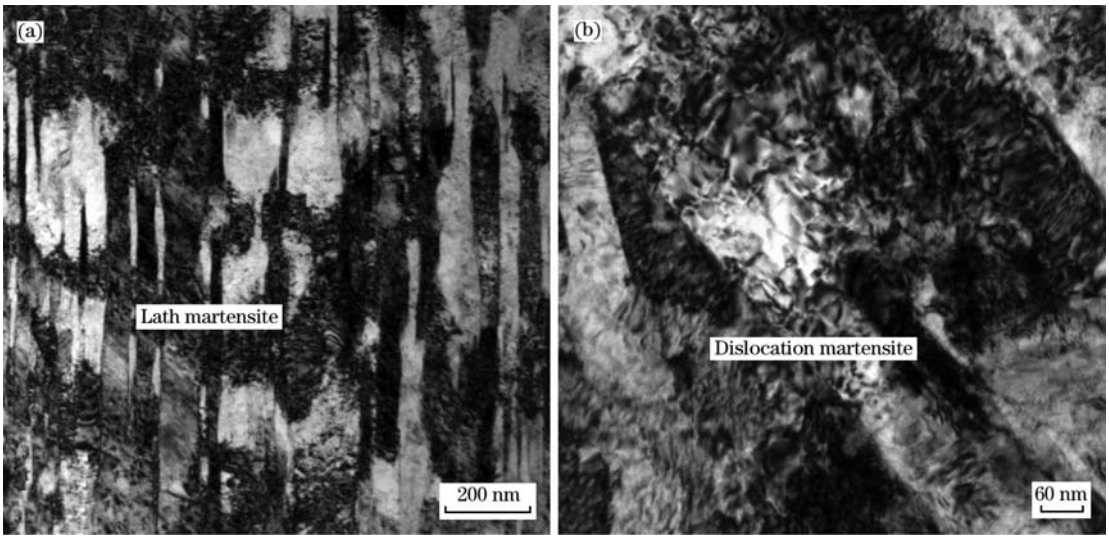

Fig. 6. TEM images of 80% cold rolled specimen showing lath-type martensite (a) and dislocation-cell type martensite (b).

thought that the two types of martensite generated concurrently in deformed specimens under saturation state; further deformation of specimens just made their volume fractions different. In this work, it seems that there are more potential nucleation sites in dislocation-cell type martensite and this dislocation-cell type martensite is essential to obtain NG/UFG austenite during reversion treatment according to the study of Rajasekhara et al.[31].

After the work of cold deformation, it is suggested that the 80% cold rolled sample is suitable for the subsequent annealing treatment. Hence, reversion process has been carried out in the 700－900 ℃ temperature. The EBSD microstructures of the sample with 80% CR annealed at 800, 850 and 900 ℃ are shown in Fig. 7. XRD analysis showed that the content of reversed austenite has been up to 99.19%, 99.51% and 100% respectively. That is to say, with the increase of annealing temperature, the content of reversed austenite is also increased. Reverted austenite with a nano/ultrafine grain-size distribution is shown in Fig. 7. At 850 ℃, the austenite grains reverse more sufficiently than at 800 ℃, and almost all the austenite grains are equiaxed. When the annealing temperature comes to 900 ℃, the austenite grains become obviously coarse.

The grain size distribution statistics have been done, as shown in Fig. 8. For the sample annealed at 800 ℃ for 60 s, the percentage of nanocrystalline (60－100 nm) and ultrafine (100－500 nm) grains accounts for 45%. The percentage of submicron size (500－1000 nm) grains accounts for 30%. And the percentage of micron size (>1000 nm) grains accounts for 25%. For the sample annealed at 850 ℃ for 60 s, the percentage of nanocrystalline/ultrafine grains accounts for 42%. The percentage of submicron

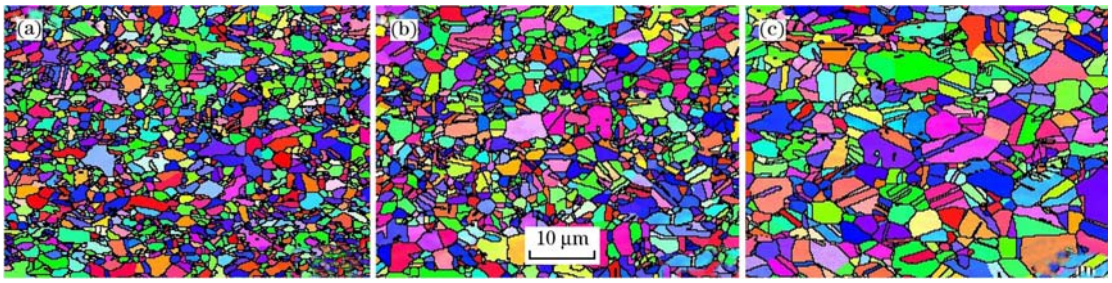

Fig. 7. EBSD microstructures of 80% rolled samples annealed at 800 ℃ (a), 850 ℃ (b), and 900 ℃ (c) for 60 s.

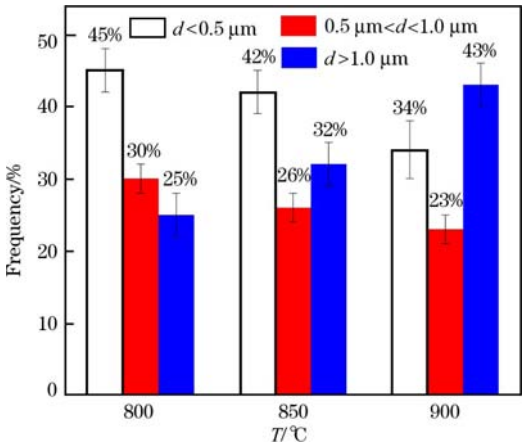

Fig. 8. Grain size distribution statistics of 80% rolled 304 SS tested at different annealing temperatures.

size grains accounts for 26%, and the percentage of micron size grains accounts for 32%. However, for the sample annealed at 900 ℃ for 60 s, the percentage of nanocrystalline/ultrafine grains accounts for 34%. The percentage of submicron size grains accounts for 23%, and the percentage of micron size grains accounts for 43%. Therefore, with the increase of annealing temperature, the percentage of ultrafine and nanocrystalline grains and submicron size grains is decreased, while the percentage of micron size grains is increased. Based on the image analysis and grain statistics, it seems that NG/UFG structure was obtained from heavy deformation and annealing treatment. Meanwhile, it confirms that heavy deformation of the specimens provides more nucleation sites, and after annealing treatment it gets much more number of austenite grains.

It was reported[27,33] that both the composition of the material and annealing temperature play the key role in whether the reversion mechanism of $\alpha'\rightarrow\gamma$ is shear controlled or diffusion controlled. Tomimura et al.[27] reported that, during the $\alpha'\rightarrow\gamma$ reversion transformation, the calculation of Gibbs free energy change is the key to determine the reversion mechanism. They held the idea that the sufficient driving force for shear controlled reversion is about －500 J/mol regardless of the composition of the material. Equation for the Gibbs free energy change $\Delta G^{\alpha'\rightarrow\gamma}$ for the $\alpha'\rightarrow\gamma$ transformation in Fe-Cr-Ni alloys was[27]:

$$\Delta G^{\alpha'\rightarrow\gamma}(\mathrm{J/mol})=10^{-2}\Delta G_{\mathrm{Fe}}^{\alpha'\rightarrow\gamma}(100-w_{\mathrm{Cr}}-w_{\mathrm{Ni}})-97.5w_{\mathrm{Cr}}+2.02w_{\mathrm{Cr}}^2-108.8w_{\mathrm{Ni}}+0.52w_{\mathrm{Ni}}^2-0.05w_{\mathrm{Cr}}w_{\mathrm{Ni}}+10^{-3}T(73.3w_{\mathrm{Cr}}-0.67w_{\mathrm{Cr}}^2+50.2w_{\mathrm{Ni}}-0.84w_{\mathrm{Ni}}^2-1.51w_{\mathrm{Cr}}w_{\mathrm{Ni}}) \quad (1)$$

where, $\Delta G_{\mathrm{Fe}}^{\alpha'\rightarrow\gamma}$ is the free energy in pure iron; T is Kelvin temperature; and w_{Cr} and w_{Ni} are mass fractions of Cr and Ni, respectively.

Later, Eq. (1) was amended and several elements were included[14], which can be

$$w_{\mathrm{Cr}}^{\mathrm{eq}}=w_{\mathrm{Cr}}+4.5w_{\mathrm{Mo}} \quad (2)$$

$$w_{\mathrm{Ni}}^{\mathrm{eq}}=w_{\mathrm{Ni}}+0.6w_{\mathrm{Mn}}+20w_{\mathrm{C}}+4w_{\mathrm{N}}-0.4w_{\mathrm{Si}} \quad (3)$$

where, $w_{\mathrm{Cr}}^{\mathrm{eq}}$ and $w_{\mathrm{Ni}}^{\mathrm{eq}}$ are the mass fractions of Cr and Ni at equilibrium state, respectively; and w_{Mo}, w_{Mn}, w_{C}, w_{N}, w_{Si} are mass fractions.

$\Delta G^{\alpha'\rightarrow\gamma}$ was finally calculated to be －553, －552 and －551 J/mol at 800, 850 and 900 ℃, respectively. The result shows that the reversion mechanism is shear reversion at these temperatures. Meanwhile, it is thought that the diffusion controlled mechanism does not exist before and after the reversion process because of the random nucleation and growth of the austenite.

Fig. 9(a) shows the TEM images of sample with cold rolling reduction of 80% after annealing at 700 ℃ for 60 s. It is found that the austenite nucleated at the place of martensite lath boundaries, as marked in Fig. 9(a), which is in agreement with the study of Misra who has reported that austenite generally nucleated at the martensite lath boundaries[32]. However, Johannsen et al.[34] have shown that dislocation cell-type martensite nucleated to austenite preferentially than that of lath-type martensite. It can be attributed to the high dislocation density of dislocation cell-type martensite which easily acts as nucleation sites for reverted austenite. As shown in Fig. 9(b), it is found that austenite nucleated on dislocation cell-type martensite in the sample annealed at 750 ℃ for 60 s. Therefore, during the $\alpha'\rightarrow\gamma$ reversion, for a certain annealing time during the reversion process, austenite nucleated first on dislocation-cell type martensite and subsequently the grains grew up, eventually to be micrometer/submicrometer grains, while

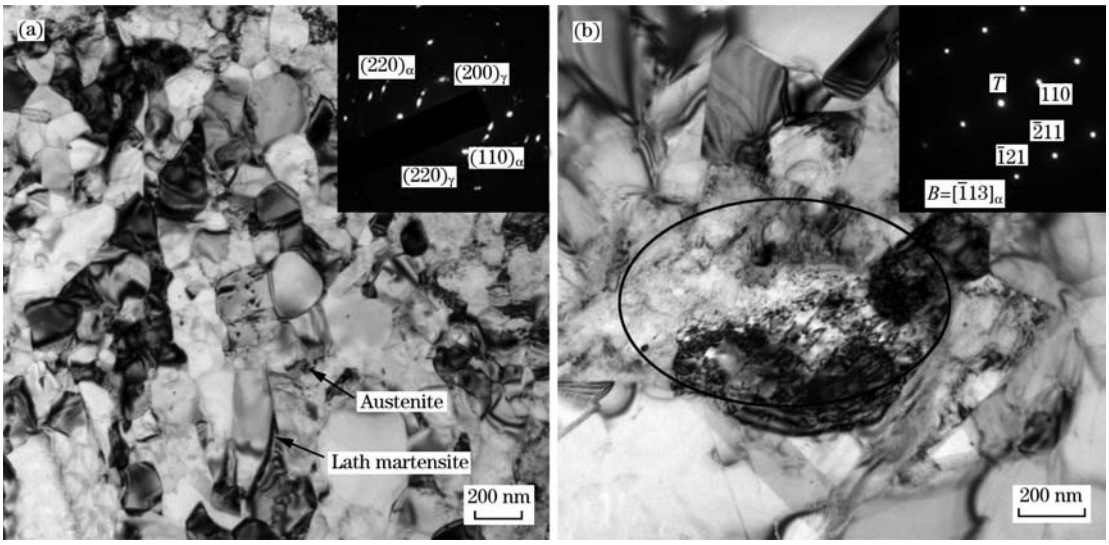

Fig. 9. TEM images of 80% cold rolled specimen annealed at 700 ℃ (a) and 750 ℃ (b).

the nucleation of austenite on lath-type martensite occurred later resulting in nanocrystalline/ultrafine grains. During the $\alpha' \rightarrow \gamma$ reversion, dislocation-cell type martensite first transformed to reverted austenite. Simultaneously, reverted austenite grew up and the content of the martensite declined. Moreover, it has reported that lath-type martensite boundaries consist of incidental dislocation boundaries (IDBs) and geometrically necessary boundaries (GNBs). The UFG grains tend to nucleate at GNBs[8,9,12]. Consequently, it is speculated that after annealing treatment of the heavy cold deformation specimen, austenite nucleates on the dislocation cell-type martensite at first. Once these nucleation centers are consumed, the austenite grains then nucleate at GNBs in lath-type martensite boundaries.

Fig. 10(a) shows the TEM images of sample with cold rolling reduction of 80% after annealing at 800 ℃ for 60 s. As shown in Fig. 10(a), the microstructure consists of very fine reverted grains with twins along with deformed austenite, while the austenite grains have defects and are not entirely equiaxed. However, when the temperature is increased up to 850 ℃, the nano/ultrafine grains are equiaxed as shown in Fig. 10(b). As shown in the picture, reverted austenite generates in martensite blocks under insufficient cold rolling. And the austenite lathes and blocks are obtained after full reversion[29].

Table 2 shows the mechanical properties of the 80% cold rolled 304 SS at different annealing temperatures. With the increase of annealing temperature, the strength and hardness are decreased, while the elongation is increased. At 700 ℃, the microstructure exhibits low elongation of 8.2%±0.3% and

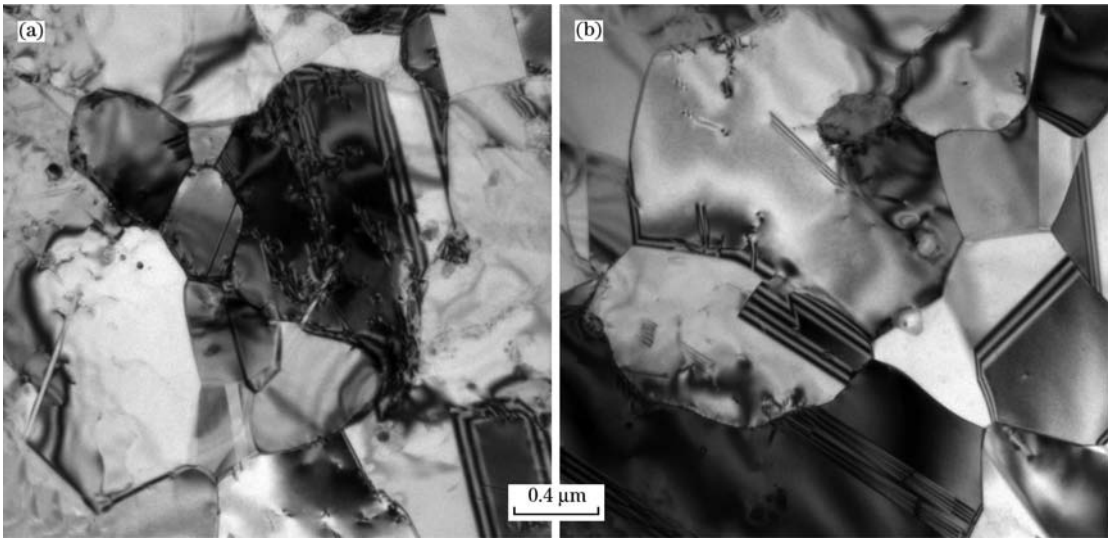

Fig. 10. TEM images of 80% cold rolled specimen annealed at 800 ℃ (a) and 850 ℃ (b).

Table 2
Mechanical properties for 80% cold rolled 304 SS tested at different annealed temperatures

T/℃	σ_t/MPa	σ_y/MPa	Elongation/%	Hardness/HV
700	1157±20	1028±14	8.2±0.3	376±5
750	883±4	562±17	43.3±2	255±4
800	867±10	522±20	49.0±1	254±3
850	861±14	474±5	51.2±1	237±4
900	843±3	408±24	59.1±2	214±2

high yield strength of (1028±14) MPa, which suggests that the reversed transformation is not complete. Also, the tensile strength decreased slightly in the 800－850 ℃ range, while the elongation to failure increased further compared to samples annealed under 800 ℃. It is suggested that grain refinement with the NG/UFG structure leads to a good combination of strength and toughness.

4. Conclusions

(1) Austenitic stainless steel tended to perform work hardening during further cold-working. The martensite nuclei were formed in the place of shear band. Further rolling broke up the lath-type martensite into dislocation-cell type martensite. These two types of martensite were important to obtain NG/UFG austenite during reversion treatment.

(2) Reversion mechanism was shear controlled annealed in the 800－900 ℃ range. For a certain annealing time during the reversion process, austenite nucleated first on dislocation-cell type martensite and subsequently the grains grew up, eventually to be micrometer/submicrometer grains, while the nucleation of austenite on lath-type martensite occurred later resulting in nanocrystalline/ultrafine grains.

(3) Microstructure with the NG/UFG structure in the 800－850 ℃ range exhibits a good combination of strength and toughness.

Acknowledgment

This research was supported by the National Natural Science Foundation of China (Grant No. 51474031).

References

[1] B. R. Kumar, S. Sharma, Metall. Mater. Trans. A 45 (2014) 6027-6038.
[2] C. Koch, Scripta Mater. 49 (2003) 657-662.
[3] E. Ma. Scripta Mater. 49 (2003) 663-668.
[4] R. D. K. Misra, K. K. Tenneti, G. C. Weatherly, G. Tither, Metall. Mater. Trans. A 34 (2003) 2341-2351.
[5] R. D. K. Misra, H. Nathani, J. E. Hartmann, F. Siciliano, Mater. Sci. Eng. A 394 (2005) 339-352.
[6] S. Shanmugam, R. D. K. Misra, T. Mannering, D. Panda, S. G. Jansto, Mater. Sci. Eng. A 437 (2006) 436-445.
[7] G. B. Olson, M. Cohen, Metall. Trans. A 6 (1975) 791-795.
[8] R. Ueji, N. Tsuji, Y. Minamino, Y. Koizumi, Acta Mater. 50 (2002) 4177-4189.
[9] N. Tsuji, R. Ueji, Y. Minamino, Y. Saito, Scripta Mater. 46 (2002) 305-310.
[10] S. Takaki, K. Tomimura, S. Ueda, ISIJ Int. 34 (1994) 522-527.
[11] D. A. Korzekwa, D. K. Matlock, G. Krauss, Metall. Trans. A 15 (1984) 1221-1228.
[12] N. Hansen, R. F. Mehl, Metall. Mater. Trans. A 32 (2001) 2917-2935.
[13] D. C. Cook, Metall. Trans. A 18 (1987) 201-210.
[14] M. C. Somani, P. Juntunen, L. P. Karjalainen, R. D. K. Misra, A. Kyröläinen, Metall. Mater. Trans. A 40 (2009) 729-744.
[15] S. Rajasekhara, P. J. Ferreira, L. P. Karjalainen, A. Kyröläinen, Metall. Mater. Trans. A 38 (2007) 1202-1210.
[16] H. Wu, G. Niu, J. Cao, M. Yang, Mater. Sci. Technol. (2016) 1-7.
[17] Y. Ma, J. Jin, Y. Lee, Scripta Mater. 52 (2005) 1311-1315.
[18] Y. Murata, S. Ohashi, Y. Uematsu, ISIJ Int. 33 (1993) 711-720.
[19] K. Tomimura, S. Takaki, S. Tanimoto, Y. Tokunaga, ISIJ Int. 31 (1991) 721-727.
[20] S. Sabooni, F. Karimzadeh, M. H. Enayati, J. Mater. Eng. Perform. 23 (2014) 1665-1672.
[21] R. N. Dehsorkhi, S. Sabooni, F. Karimzadeh, A. Rezaeian, M. H. Enayati, Mater. Des. 64 (2014) 56-62.
[22] A. Momeni, S. M. Abbasi, J. Mater. Process. Technol. 27 (2011) 338-343.
[23] A. Hedayati, A. Najafizadeh, A. Kermanpur, F. Forouzan, J. Mater. Process. Technol. 210 (2010) 1017-1022.
[24] F. Forouzan, A. Najafizadeh, A. Kermanpur, A. Hedayati, R. Surkialiabad, Mater. Sci. Eng. A 527 (2010) 7334-7339.
[25] V. S. A. Challa, X. L. Wan, M. C. Somani, L. P. Karjalainen, R. D. K. Misra, Mater. Sci. Eng. A 613 (2014) 60-70.
[26] Y. M. Wang, E. Ma, Acta Mater. 52 (2004) 1699-1709.
[27] K. Tomimura, S. Takaki, Y. Tokunaga, ISIJ Int. 31 (1991) 1431-1437.
[28] W. S. Lee, C. F. Lin, Scripta Mater. 43 (2000) 777-782.
[29] S. Sabooni, F. Karimzadeh, M. H. Enayati, A. H. W. Ngan, Mater. Sci. Eng. A 636 (2015) 221-230.
[30] R. D. K. Misra, J. S. Shah, S. Mali, P. K. C. V. Surya, M. C. Somani, L. P. Karjalainen, Mater. Sci. Technol. 29 (2013) 1185-1192.
[31] S. Rajasekhara, L. P. Karjalainen, A. Kyröläinen, P. J. Ferreira, Mater. Sci. Eng. A 527 (2010) 1986-1996.
[32] R. D. K. Misra, S. Nayak, S. A. Mali, J. S. Shah, M. C. Somani, L. P. Karjalainen, Metall. Mater. Trans. A 40 (2009) 2498-2509.
[33] P. Behjati, A. Kermanpur, A. Najafizadeh, H. S. Baghbadorani, Mater. Sci. Eng. A 592 (2014) 77-82.
[34] D. L. Johannsen, A. Kyrolainen, P. J. Ferreira, Metall. Mater. Trans. A 37 (2006) 2325-2338.